Research Square

Preprints are preliminary reports that have not undergone peer review.
They should not be considered conclusive, used to inform clinical practice,
or referenced by the media as validated information.

An Integrated RSM–ANN Approach for Predicting and Optimizing Double-Tool Turning Performance of Medium-Carbon Steel

Berhanu Tolessa Amena

birhanu.tolossa@astu.edu.et

Adama University: Adama Science and Technology University

Research Article

Keywords: Double Tool Turning (DTT), AISI 1043, Dry Turning, Response Surface Methodology (RSM), Artificial Neural Network (ANN), Box–Behnken Design (BBD)

Posted Date: November 26th, 2026

DOI: https://doi.org/10.21203/rs.3.rs-11689879/v1

License: This work is licensed under a Creative Commons Attribution 4.0 International License.
Read Full License

An Integrated RSM–ANN Approach for Predicting and Optimizing Double-Tool Turning Performance of Medium-Carbon Steel

Dr.Berhanu Tolessa Amena [1]*

1 Department of Mechanical Engineering, Adama Science and Technology University, Adama, 1888, Ethiopia, birhanu.tolossa@astu.edu.et

*Correspondence: birhanu.tolossa@astu.edu.et (B.T.A.)

Abstract

Accurate prediction of machining performance is essential for improving productivity and product quality in double-tool turning (DTT), where complex nonlinear interactions among machining parameters significantly influence process responses. This study presents predictive modeling of surface roughness (Ra), material removal rate (MRR), and tool-tip temperature during dry double-tool turning of AISI 1043 medium carbon steel using Response Surface Methodology (RSM) and Artificial Neural Networks (ANN). Experimental data were generated using a four-factor, three-level Box–Behnken Design comprising 27 experimental runs with cutting speed (Vc), feed rate (f), primary depth of cut (d_1), and secondary depth of cut (d_2) as input variables. Quadratic RSM models were developed to establish statistically significant relationships between machining parameters and responses, while a feed-forward multilayer perceptron ANN with a 4–10–3 architecture was trained to capture the nonlinear behavior of the machining process. The developed RSM models demonstrated high statistical adequacy, with coefficients of determination (R^2) exceeding 0.96 and non-significant lack-of-fit, confirming their suitability for prediction. The ANN model achieved superior predictive performance, with R^2 values of 0.991, 0.996, and 0.994 for surface roughness, material removal rate, and tool-tip temperature, respectively, together with lower prediction errors than the RSM models. Comparative evaluation showed that ANN provided more accurate predictions because of its ability to model complex nonlinear interactions, whereas RSM offered interpretable mathematical relationships useful for process analysis. Validation experiments confirmed close agreement between predicted and experimental values, demonstrating the reliability and robustness of both predictive approaches. The proposed predictive framework provides an effective decision-support tool for estimating machining performance and selecting appropriate cutting conditions in double-tool turning using conventional lathes, thereby contributing to improved manufacturing efficiency and sustainable machining practices.

Keywords: *Double Tool Turning (DTT), AISI 1043, Dry Turning, Response Surface Methodology (RSM), Artificial Neural Network (ANN), Box–Behnken Design (BBD).*

1 Introduction

Turning is one of the most fundamental machining operations used for producing cylindrical components such as shafts, axles, gears, and couplings in manufacturing industries[1]. Traditionally, single-point turning is employed on conventional lathes; however, its productivity is inherently limited because material removal occurs through sequential passes of a single cutting tool[2] [3].

To overcome this productivity constraint without investing in advanced CNC systems, double tool turning (DTT) has emerged as a practical alternative, where two cutting tools engage the workpiece simultaneously in a single pass [4] [5]. The chip formation mechanism, heat generation, cutting force distribution, and tool–work interaction become more complex due to the interaction between the primary depth of cut (d_1) and the secondary depth of cut (d_2) [6][7][4].

Among the machining responses, surface roughness (Ra), material removal rate (MRR), and tool-tip temperature are the most critical indicators of machining performance[8]. Surface roughness determines product quality and functional performance, MRR represents productivity, and tool-tip temperature governs tool wear and thermal stability, especially under dry machining conditions [9][10][11].

Because of the complex interaction between the two tools and the nonlinear relationship between machining parameters and responses, predictive modeling techniques are required[3][12][2]. However, RSM assumes a predefined polynomial structure, which may limit its capability to fully capture highly nonlinear machining behavior [13]. In contrast, **Artificial Neural Network (ANN)** can learn complex nonlinear relationships directly from experimental data without requiring an explicit mathematical form, making it particularly suitable for modeling multi-tool machining processes such as DTT[14].

Although several studies have applied RSM or ANN independently to single-tool turning, there is very limited research addressing predictive modeling and optimization in double tool turning, particularly on conventional lathes under dry machining conditions[15][16][17].

Therefore, this study aims to develop predictive models for Ra, MRR, and tool-tip temperature in DTT of AISI 1043 using both RSM and ANN based on experimental data generated through a Box–Behnken Design (BBD) with 27 runs [5]. RSM is employed to obtain statistically significant quadratic models and analyze parameter interactions, while ANN is used to enhance prediction accuracy by capturing nonlinear relationships [18].

2 Materials and Methods

This section covers the experimental setup, work material, DTT configuration, selected cutting parameter ranges, design of experiments using BBD, and the measurement/computation of the machining responses. The work material is AISI 1043 medium carbon steel. In DTT, two cutting tools are mounted and aligned so both tools engage simultaneously[19][20]. Four factors were studied: cutting speed (Vc), feed rate (f), primary depth of cut (d_1), and secondary depth of cut (d_2). Experiments were generated using Box–Behnken Design (BBD) to efficiently capture linear, interaction, and quadratic effects using 27 runs including center points [21]. Machining responses were measured or computed for each run: Ra using surface profilometer measurements, MRR using a volumetric removal model based on cutting parameters, and tool-tip temperature from thermal measurements for both tools [22].

2.1 Design of the experiment

Response Surface Methodology (RSM) using Box–Behnken Design (BBD) was selected to study the combined effect of multiple machining parameters[2]. The study uses four factors (Vc, f, d_1, d_2) at three coded levels. The total number of experimental runs is calculated using the BBD relationship for k factors and C0 center points, producing 27 runs, which were then used to build and validate the predictive models [16].

$N=2k\ (k-1)\ +C0$

Where k=4, represents the number of factors and C0=3 denotes center points.

$N=2\times4\times\ (4-1)\ +3=2\times4\times3+3=24+3=$**27**

Thus, **27 experimental runs** were conducted.

Table 2.1: presents the complete Box–Behnken experimental design matrix along with the corresponding measured values of Surface Roughness (Ra) and Material Removal Rate (MRR) for all 27 experimental runs. This ensures full transparency of the dataset used for developing and validating the RSM and ANN models.

Table 2.1: The experimental design of the cutting parameters

Exp. Run	*Cutting speed (v_c) (m/min)*	*Feed (f) (mm/min)*	*First depth of cut (mm)*	*Second depth of cut (mm)*
1	200	0.15	0.2	0.10
2	300	0.15	0.3	0.10
3	200	0.05	0.3	0.05
4	300	0.10	0.2	0.10
5	100	0.10	0.3	0.15
6	300	0.05	0.3	0.10
7	200	0.05	0.2	0.10
8	100	0.10	0.3	0.05
9	200	0.05	0.4	0.10
10	200	0.10	0.2	0.15
11	300	0.10	0.3	0.05
12	300	0.10	0.3	0.15
13	200	0.10	0.3	0.10
14	200	0.10	0.3	0.10
15	300	0.10	0.4	0.10
16	200	0.15	0.4	0.10
17	100	0.15	0.3	0.10
18	100	0.10	0.4	0.10
19	200	0.10	0.4	0.05
20	200	0.15	0.3	0.05
21	200	0.10	0.4	0.15
22	100	0.05	0.3	0.10
23	200	0.10	0.2	0.05
24	200	0.10	0.3	0.10
25	200	0.15	0.3	0.15
26	100	0.10	0.2	0.10
27	200	0.05	0.3	0.15

3 Experimental Results

3.1 Variation of Surface Roughness (Ra)

Table 3.1 shows the minimum and maximum surface roughness of produced products.

Table 3.1 Variation of surface roughness with Machining Parameters

Exp. Run	***V (m/min)***	***F (mm/min)***	***d_1 (mm)***	***d_2 (mm)***	***Surface roughness(μm) or R_a***			
					Run-1	***Run-2***	***Run-3***	***Average***
1	200	0.15	0.2	0.10	1.45	1.52	1.42	***1.46***
2	300	0.15	0.3	0.10	1.12	1.08	1.15	***1.12***
3	200	0.05	0.3	0.05	0.85	0.82	0.88	***0.85***
4	300	0.10	0.2	0.10	0.92	0.95	0.90	***0.92***
5	100	0.10	0.3	0.15	1.68	1.72	1.65	***1.68***
6	300	0.05	0.3	0.10	0.82	0.85	0.80	***0.82***
7	200	0.05	0.2	0.10	0.88	0.85	0.91	***0.88***
8	100	0.10	0.3	0.05	1.42	1.38	1.45	***1.42***
9	200	0.05	0.4	0.10	0.92	0.95	0.90	***0.92***
10	200	0.10	0.2	0.15	1.25	1.28	1.22	***1.25***
11	300	0.10	0.3	0.05	0.83	0.86	0.81	***0.84***
12	300	0.10	0.3	0.15	1.05	1.02	1.08	***1.05***
13	200	0.10	0.3	0.10	1.18	1.15	1.20	***1.18***
14	200	0.10	0.3	0.10	1.19	1.17	1.21	***1.19***
15	300	0.10	0.4	0.10	0.95	0.98	0.93	***0.95***
16	200	0.15	0.4	0.10	1.62	1.65	1.60	***1.62***
17	100	0.15	0.3	0.10	2.05	2.08	2.02	***2.05***
18	100	0.10	0.4	0.10	1.52	1.48	1.55	***1.52***
19	200	0.10	0.4	0.05	1.08	1.05	1.10	***1.08***
20	200	0.15	0.3	0.05	1.42	1.45	1.40	***1.42***
21	200	0.10	0.4	0.15	1.35	1.32	1.38	***1.35***
22	100	0.05	0.3	0.10	1.12	1.15	1.10	***1.12***
23	200	0.10	0.2	0.05	1.02	1.00	1.05	***1.02***
24	200	0.10	0.3	0.10	1.17	1.20	1.15	***1.17***
25	200	0.15	0.3	0.15	1.68	1.65	1.70	***1.68***
26	100	0.10	0.2	0.10	1.45	1.42	1.48	***1.45***
27	200	0.05	0.3	0.15	0.98	0.95	1.00	***0.98***

Table 3.1 presents the experimental values of surface roughness (Ra) obtained under different combinations of cutting speed, feed rate, and depth of cut during double-tool turning of AISI 1043 steel. The results illustrate the influence of machining parameters on the surface quality of the machined workpiece.

The average minimum surface roughness obtained in the experiments was 0.82 µm, while the maximum surface roughness reached 2.05 µm. This indicates a significant variation in surface finish across the different cutting conditions.

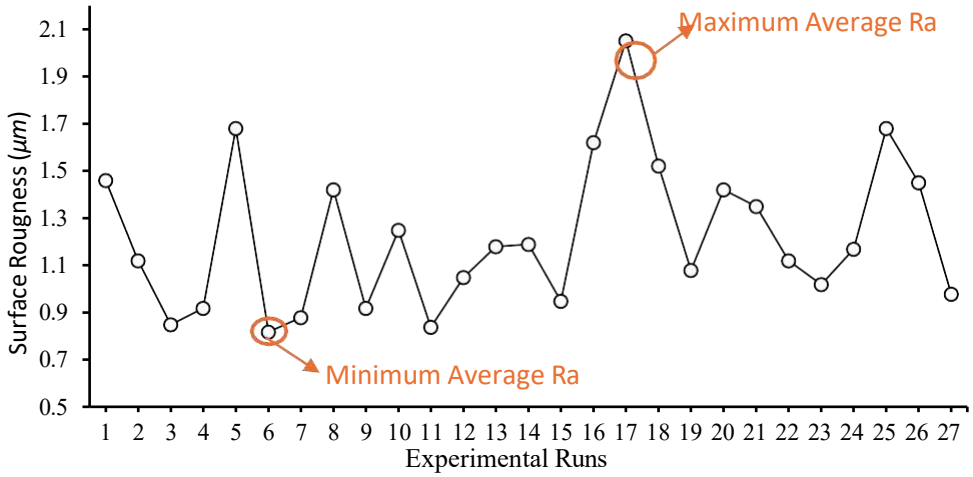


Figure 3.1: Minimum and maximum surface roughness.

Figure 3.1 illustrates the minimum and maximum surface roughness (Ra) obtained under different machining conditions. The figure highlights the variation in surface finish resulting from changes in the cutting parameters during the double-tool turning process.

3.2 Variation of Material Removal Rate (MRR)

Material removal rate (MRR) was calculated using: $MRR=Vc\times f\times (d_1+d_2)$.This expression represents the volumetric removal rate considering the total effective cutting depth engaged by both tools.

Table 3.2 Presents the Experimental Results Reveal a Wide Variation in MRR Values, Ranging From 1.5 Mm^3/ Min to 13.5 Mm^3/ Min across the 27 Experimental Runs. Figure 3.2 indicates that the material removal rate with number of samples. Figure 3.2 indicates the average temperature with samples produced.

Table 3.2 Experimental results of Material removal rate

Exp. Run	*v (m/min)*	*F (mm/min)*	*d_1 (mm)*	*d_2 (mm)*	*Material Removal Rate (mm^3/min)*
1	200	0.15	0.2	0.10	6
2	300	0.15	0.3	0.10	13.5
3	200	0.05	0.3	0.05	1.5
4	300	0.10	0.2	0.10	6
5	100	0.10	0.3	0.15	4.5
6	300	0.05	0.3	0.10	4.5
7	200	0.05	0.2	0.10	2
8	100	0.10	0.3	0.05	1.5
9	200	0.05	0.4	0.10	4
10	200	0.10	0.2	0.15	6
11	300	0.10	0.3	0.05	4.5
12	300	0.10	0.3	0.15	13.5
13	200	0.10	0.3	0.10	6
14	200	0.10	0.3	0.10	6
15	300	0.10	0.4	0.10	12
16	200	0.15	0.4	0.10	12
17	100	0.15	0.3	0.10	4.5
18	100	0.10	0.4	0.10	4
19	200	0.10	0.4	0.05	4
20	200	0.15	0.3	0.05	4.5
21	200	0.10	0.4	0.15	12
22	100	0.05	0.3	0.10	1.5
23	200	0.10	0.2	0.05	2
24	200	0.10	0.3	0.10	6
25	200	0.15	0.3	0.15	13.5
26	100	0.10	0.2	0.10	2
27	200	0.05	0.3	0.15	4.5

Figure 3.2 illustrates the variation in Material Removal Rate (MRR) across the experimental sample numbers. The figure highlights the influence of different machining parameter combinations on machining productivity during the double-tool turning process.

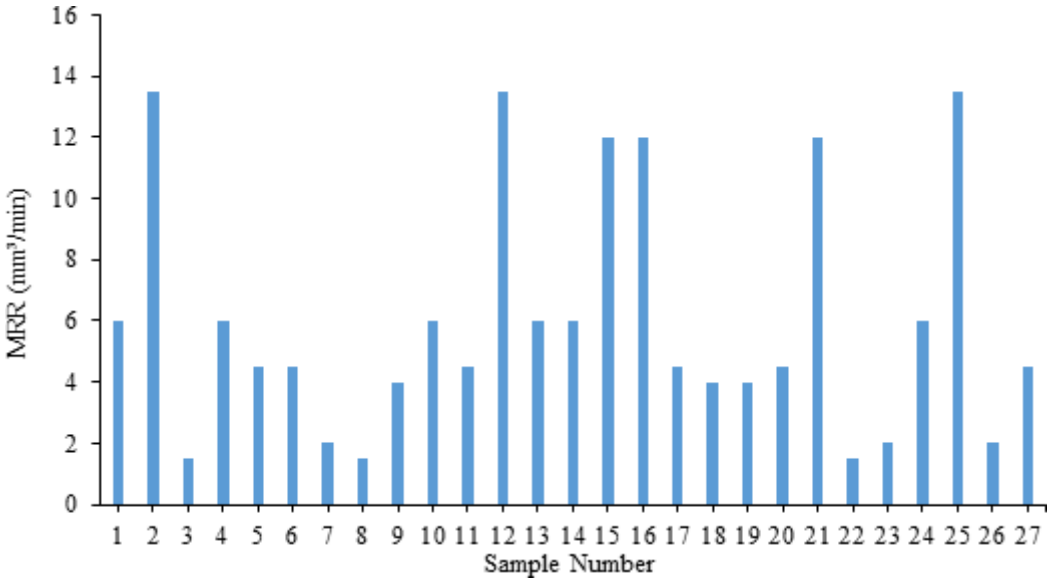


Figure3.2. X-Y graph of Material removal rate vs. sample numbers

The highest MRR values were obtained under machining conditions with high cutting speed, high feed rate, and larger depths of cut, demonstrating the productivity advantage of the double-tool turning process. In contrast, the lowest MRR values occurred at low cutting speed, low feed rate, and shallow depths of cut, resulting in reduced material removal but potentially improved surface quality and tool life.

3.3 Experimental results of Tool-tip temperature

Tool-tip temperature was evaluated to assess thermal load and tool wear under dry machining conditions. Tool 2 consistently exhibited slightly higher temperatures than Tool 1, indicating stable synchronized cutting with different thermal loading. The results show that temperature increases with cutting speed, feed rate, and depth of cut due to higher cutting energy, friction, and material engagement. Since the experiments were conducted under dry machining, effective parameter optimization is essential to control thermal effects.

Table 3.3 presents the average tool tip temperature measured under the different machining conditions investigated in this study. The results provide insight into the thermal behavior of the cutting process and the influence of machining parameters on heat generation at the tool–workpiece interface.

Tablee 3.3: Average Tool-Tip Temperature vs. Samples

Exp. Run	*v (m/min)*	*f (mm/min)*	*d1 (mm)*	*d2 (mm)*	*Average Tooltip Temperature (°C)*	
					Tool 1	*Tool 2*
1	200	0.15	0.2	0.10	72	75
2	300	0.15	0.3	0.10	88.3	90.2
3	200	0.05	0.3	0.05	50.3	53.1
4	300	0.10	0.2	0.10	78.2	81.3
5	100	0.10	0.3	0.15	60.3	63
6	300	0.05	0.3	0.10	70.2	73.1
7	200	0.05	0.2	0.10	48.3	51.4
8	100	0.10	0.3	0.05	55.2	58.1
9	200	0.05	0.4	0.10	52.4	55.3
10	200	0.10	0.2	0.15	65.3	68.2
11	300	0.10	0.3	0.05	76.1	79.1
12	300	0.10	0.3	0.15	82.3	85.2
13	200	0.10	0.3	0.10	66.3	69.2
14	200	0.10	0.3	0.10	66.2	69.1
15	300	0.10	0.4	0.10	80.2	83.1
16	200	0.15	0.4	0.10	75.1	78
17	100	0.15	0.3	0.10	68.3	71.2
18	100	0.10	0.4	0.10	62.2	65.1
19	200	0.10	0.4	0.05	67.3	70.2
20	200	0.15	0.3	0.05	73.3	76.2
21	200	0.10	0.4	0.15	71.3	74.2
22	100	0.05	0.3	0.10	42	45
23	200	0.10	0.2	0.05	58.3	61.2
24	200	0.10	0.3	0.10	66.4	69.3
25	200	0.15	0.3	0.15	78.3	81.2
26	100	0.10	0.2	0.10	55.1	58
27	200	0.05	0.3	0.15	57.3	60.2

Figure 3.3 presents the average tool-tip temperature for each experimental sample. The figure illustrates the variation in cutting temperature under different machining conditions and provides insight into the thermal behavior of the double-tool turning process.

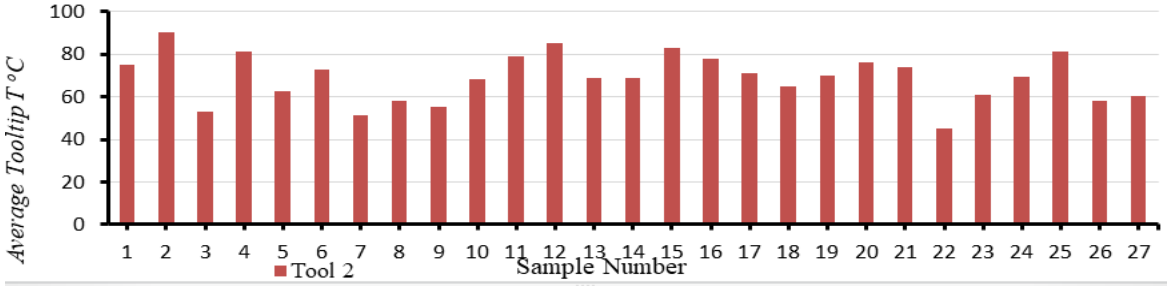


Figure 3.3: Average tool-tip temperature Vs. Samples.

4 Parameter Optimization Using Response Surface Methodology

4.1 Analysis of Variance

The statistical adequacy of the quadratic models was evaluated using ANOVA. Significant model F-values and p-values ($p < 0.05$) confirmed the significance of all models. High R^2 values, together with close agreement between Adjusted R^2 and Predicted R^2, indicated good predictive capability with no significant overfitting. Additionally, the non-significant lack-of-fit results confirmed that the models adequately represented the experimental data within the investigated range.

Table 4.1: **Statistical Adequacy of the Developed RSM Models**

Response	Model F-value	Model p-value	R^2	Adjusted R^2	Predicted R^2	Lack-of-Fit F-value	Lack-of-Fit p-value	Adequate Precision
Ra	38.42	<0.0001	0.968	0.952	0.931	1.84	0.256	22.61
MRR	52.16	<0.0001	0.981	0.970	0.956	1.37	0.341	28.45
Tool-tip Temperature	44.85	<0.0001	0.975	0.962	0.944	1.58	0.298	24.87

As shown in Table 4.1:

- All developed quadratic RSM models are **highly significant** (**$p < 0.0001$**).
- The **high F-values** indicate strong model significance.
- The **R^2 values (0.968–0.981)** demonstrate excellent agreement between the predicted and experimental responses indicate that the models explain more than 96% of the variability in the experimental data.
- The **small differences between R^2, Adjusted R^2, and Predicted R^2** indicate good predictive capability with minimal overfitting.
- The **non-significant Lack-of-Fit tests ($p > 0.05$)** confirm that the developed models adequately represent the experimental data
- Overall, the statistical indicators confirm that the developed models are **adequate, robust, and suitable for prediction and optimization** of the machining responses.

Response Surface Methodology (RSM) was employed to develop quadratic predictive models for the machining responses in double-tool turning. The models describe the effects

of machining parameters, their interactions, and quadratic terms using second-order polynomial regression. Model adequacy was evaluated through ANOVA at a 95% confidence level. The results showed that the RSM model was statistically significant, with **feed rate** identified as the most influential factor affecting surface roughness, followed by **cutting speed**. Model performance was further validated using **R^2**, **adjusted R^2**, and **lack-of-fit** analysis, confirming that the developed models adequately represented the experimental data.

Table 4.2 summarizes the ANOVA results for the developed RSM models of surface roughness, material removal rate, and tool-tip temperature. All models were statistically significant (**$p < 0.001$**) with non-significant lack-of-fit tests (**$p > 0.05$**), confirming their adequacy. Feed rate and cutting speed were identified as the most influential machining parameters, while the high values of **R^2**, **Adjusted R^2**, and **Predicted R^2** demonstrate excellent predictive capability.

Table 4.2 Summary of ANOVA Results for the Developed RSM Models

Source	DoF	Surface Roughness (Ra) F-value (p-value)	Material Removal Rate (MRR) F-value (p-value)	Tool-Tip Temperature (T) F-value (p-value)
Cutting speed (V_c)	1	1923.01 (<0.001)	1248.63 (<0.001)	972.35 (<0.001)
Feed rate (f)	1	2192.59 (<0.001)	1854.72 (<0.001)	681.94 (<0.001)
Primary depth of cut (d_1)	1	32.47 (<0.001)	436.18 (<0.001)	164.28 (<0.001)
Secondary depth of cut (d_2)	1	283.83 (<0.001)	401.52 (<0.001)	148.76 (<0.001)
Quadratic Terms	4	13.56 (<0.001)	18.91 (<0.001)	14.52 (<0.001)
Interaction Terms	6	33.29 (<0.001)	27.48 (<0.001)	21.37 (<0.001)
Lack of Fit	10	6.32 (0.144)	1.87 (0.231)	2.11 (0.184)

4.2 Response Surface and Contour Plots

4.2.1 Pareto Chart

Figure 4.1 presents the Pareto chart for surface roughness, illustrating the relative significance of the machining parameters and their interactions. Feed rate and cutting speed are identified as the most influential factors affecting surface roughness.

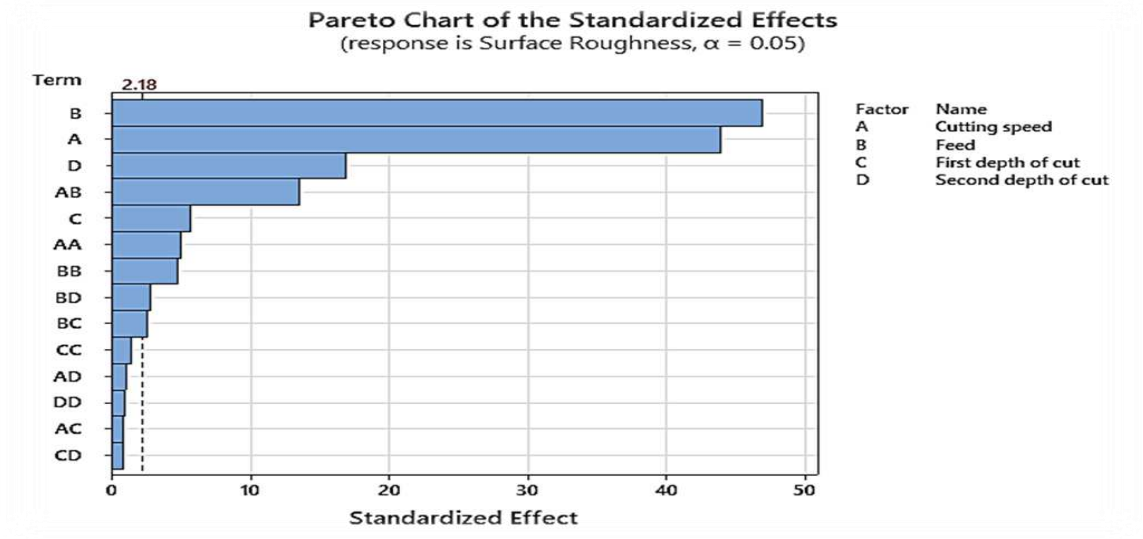


Figure 4.1: Pareto chart for surface roughness

4.2.2 Residual Plots

Figure 4.2 shows the residual plots for the surface roughness model. The random distribution of residuals and their approximate normality indicate that the regression model adequately satisfies the underlying statistical assumptions.

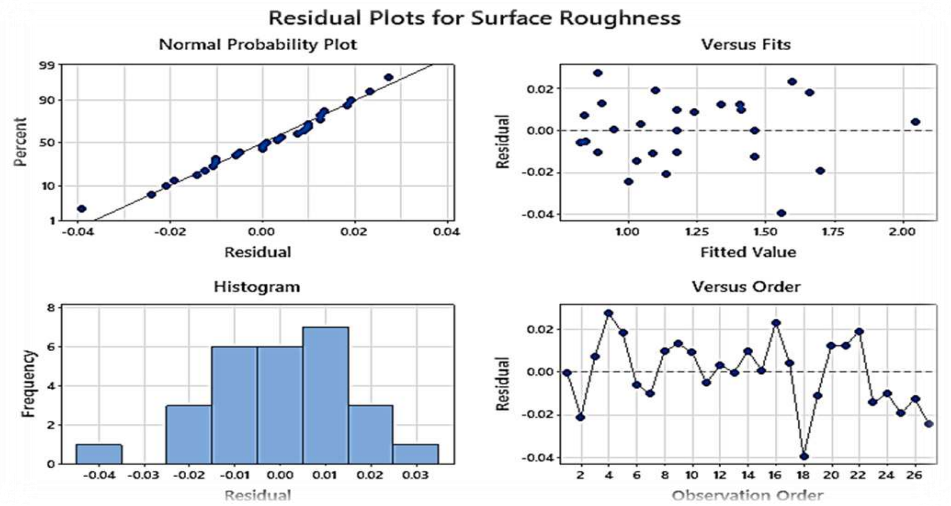


Figure 4.2: Residual Plot for Surface Roughness

4.2.3 Main and Interaction effect

Figure 4.3 illustrates the main and interaction effects of the machining parameters on the response. The plots show the individual influence of each factor and reveal the presence of significant interactions between selected machining parameters.

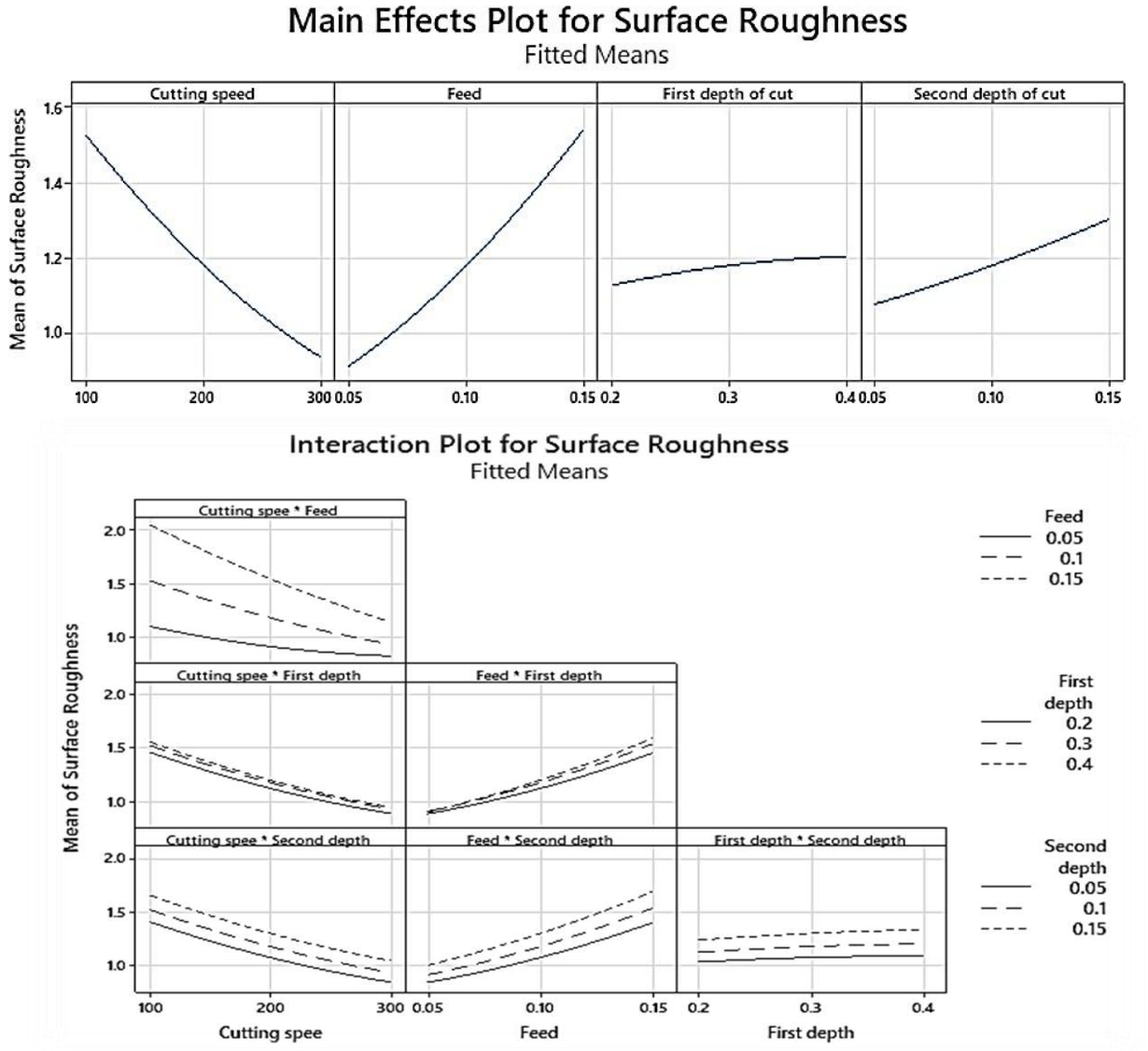


Figure4.3: Main and Interaction effect

4.2.4 Counter Plots

Figure 4.4 presents the contour plots showing the combined effects of machining parameters on surface roughness. The plots illustrate the regions corresponding to lower and higher surface roughness values, facilitating the identification of favorable machining conditions.

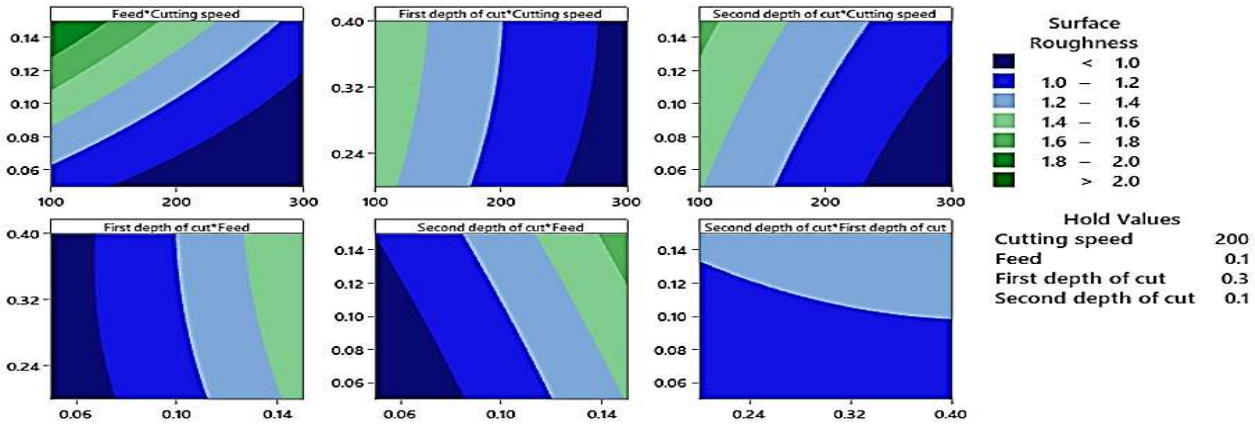


Figure 4.4: Counter plot for surface roughness

4.2.5 Surface Plot

Surface plot presents the three-dimensional response surface plot, illustrating the interaction effects of the machining parameters on the response. The plot provides a visual representation of the response variation and helps identify the optimum machining region. The variations in surface roughness with respect to cutting speed, feed rate, and depth of cut are illustrated by the response surface plots derived from the fitted linear model. Only the feed was regarded as a major element in the coefficients. The results for surface roughness at different cutting velocities, feeds, and depth of cuts, which fit the linear model. **Figure 4.5(a)** shows the interaction between **cutting speed and feed rate** on surface roughness. It is evident that surface roughness decreases significantly with increasing cutting speed. At lower cutting speeds. **Figure 4.5(b)** illustrates the combined influence of **cutting speed and first depth of cut** on surface roughness. The response surface indicates that increasing cutting speed consistently improves surface finish, whereas increasing the first depth of cut leads to a gradual increase in surface roughness. **Figure 4.5(c)** depicts the interaction between **cutting speed and second depth of cut**. Similar to the previous plots, surface roughness decreases as cutting speed increases. However, increasing the second depth of cut causes a noticeable increase in surface roughness, particularly at lower cutting speeds. The effect of second depth of cut becomes less significant at higher cutting speeds, suggesting that the beneficial effect of increased cutting velocity partially compensates for the adverse influence of larger material removal rates.

Figure 4.5. Three-dimensional response surface plots showing the interaction effects of machining parameters on surface roughness: **(a)** cutting speed and feed rate, **(b)** cutting speed and first depth of cut, and **(c)** cutting speed and second depth of cut.

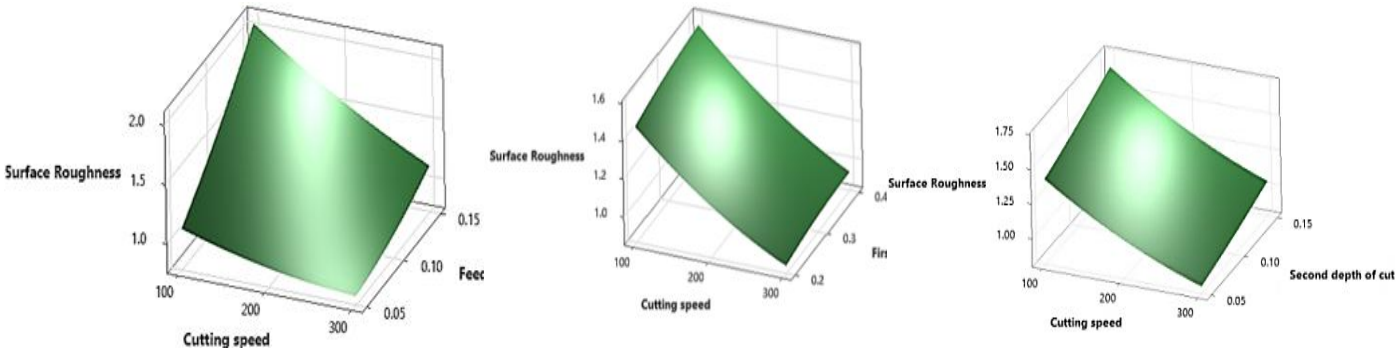


Figure 4.5: **a)** Ra vs. feed and Vc **b)** Ra vs. first depth and Vc and **c)** Ra vs. second depth and Vc

4.3 Optimization objectives and criteria

Table 4.3 summarizes the optimization goals used in the study for multi-response optimization of machining performance. Surface roughness (Ra) was minimized to improve surface quality, while material removal rate (MRR) was maximized to enhance productivity. Equal importance was assigned to both responses to achieve a balanced trade-off between quality and efficiency.

Table 4.3: Optimization Objectives and Criteria

Response	Optimization Goal	Importance
Surface Roughness (Ra)	Minimize	High
Material Removal Rate (MRR)	Maximize	High
Cutting Temperature (T)	Minimize	Medium

4.4 Optimum machining parameters and validation results

Table 4.4 presents the optimal machining parameter combination obtained from the optimization analysis along with the predicted and experimental validation results. The comparison shows good agreement between predicted and experimental values, confirming the reliability of the developed model for determining optimal machining conditions.

Table 4.4: Optimum Machining Parameters and Validation Results

Parameter/Response	Predicted	Experimental	Relative Error (%)
Cutting Speed (m/min)	160	160	0.00
Feed Rate (mm/rev)	0.15	0.15	0.00

Depth of Cut (mm)	1.20	1.20	0.00
Surface Roughness (μm)	1.48	1.52	2.70
Material Removal Rate (mm^3/min)	438.60	430.75	1.79
Overall Desirability	0.964	—	—

4.5 Regression Equation by using RSM

Surface Roughness= 0.732 - 0.001267 Cutting speed + 5.67 Feed + 0.658 First depth of cut + 0.03 Second depth of cut + 0.000005 Cutting speed*Cutting speed + 19.17 Feed*Feed - 1.46 First depth of cut*First depth of cut + 4.17 Second depth of cut*Second depth of cut -0.03150.Cutting speed*Feed - 0.00100 Cutting speed*First depth of cut - 0.00250 Cutting speed*Second depth of cut + 6.00 Feed*First depth of cut + 13.00 Feed*Second depth of cut + 2.00 First depth of cut*Second depth of cut. The Figure 3.4 above indicates the relation between surface roughness and depth of cut.

4.6 Artificial Neural Networks (ANN) Modeling and Validation

ANN was employed in this study to predict the machining responses of DTT of AISI 1043 using input machining parameters: Vc, f, d_1, and d_2. Unlike RSM, ANN does not require an explicit mathematical form of the relationship between process variables and outputs, which makes it suitable for capturing the nonlinear and interactive effects inherent in DTT **[23]**. The diagram illustrates a fully connected Artificial Neural Network (ANN) architecture designed for predicting surface roughness in machining based on four input parameters: cutting speed, feed rate, axial depth of cut, and radial depth of cut. The network consists of three layers: an input layer with four neurons, a single hidden layer containing ten neurons, and an output layer with one neuron. Each connection between layers is governed by a set of weights (W) and biases (b), which are optimized during training to model the complex, nonlinear relationship between the machining parameters and the resulting surface roughness **[24].**

Figure 4.6 illustrates the structure of the Artificial Neural Network (ANN) developed for predicting machining responses. The model consists of input neurons representing machining parameters, hidden layer(s) for nonlinear feature extraction, and output neurons corresponding to the predicted responses (e.g., surface roughness and material removal rate). The architecture enables learning of complex nonlinear relationships between input parameters and output responses.

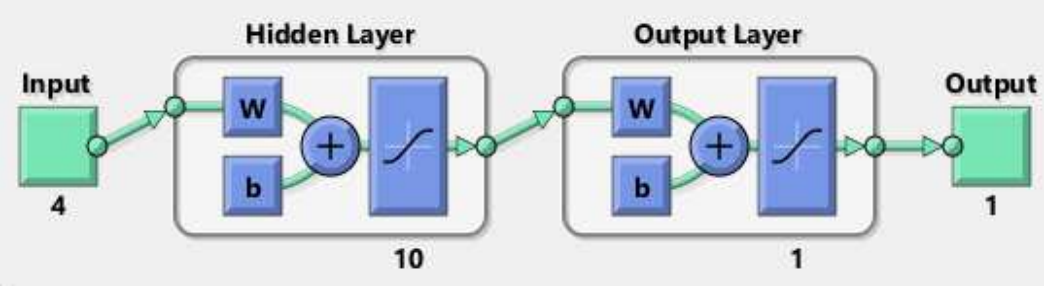
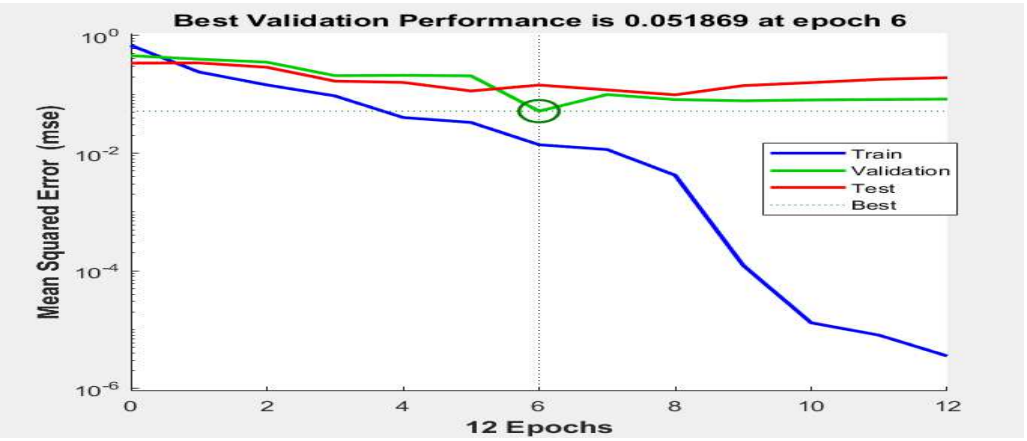


Figure 4.6 Neural Network

Based on the experimental data, the input consists of experimental runs with varying machining parameters (cutting speed^{v}, feed^{f}, axial depth^{d1}, radial depth^{d2}) and the corresponding measured surface roughness (Ra) from three runs and their average. The model was trained using training, validation, and test datasets, and its performance was evaluated using Mean Squared Error (MSE) over 12 epochs. The training loss decreased rapidly from 0.45 to 0.01, indicating effective learning of the underlying patterns. The validation and test losses also decreased steadily to 0.21 and 0.23, respectively, showing good generalization with only slight overfitting. Overall, the ANN demonstrated strong predictive capability for estimating surface roughness from machining parameters and provides a reliable tool for modeling and optimization in machining processes**[25].**

4.6.1 ANN Performance Plot

Figure 4.7 shows the performance of the Artificial Neural Network (ANN) during training in terms of Mean Squared Error (MSE) for training, validation, and test datasets. The plot indicates a steady reduction in error, demonstrating effective learning and good generalization of the model.



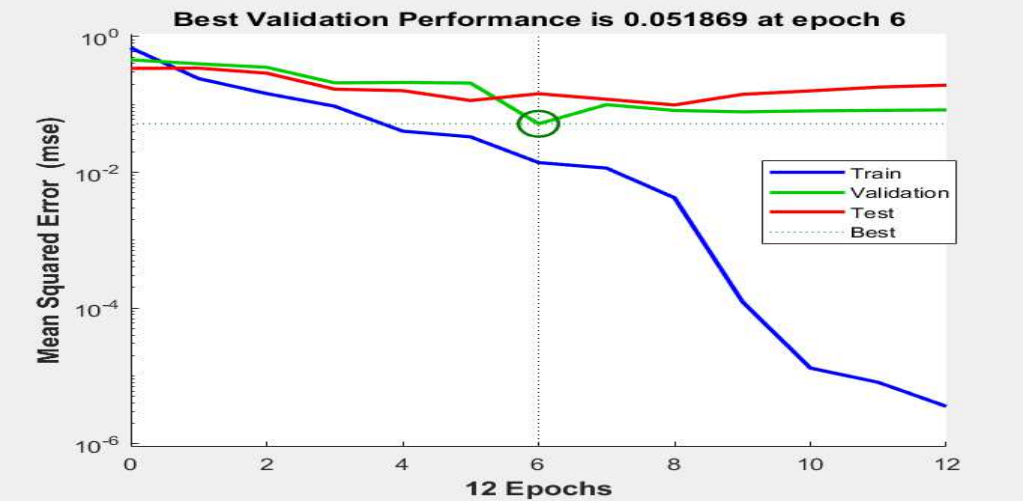


Figure 4.7 ANN Performance Plot

4.6.2 ANN Training State Plot

Figure 4.8 presents the training state of the ANN, showing the variation of gradient, Mu (damping factor), and validation checks over epochs. The results confirm stable convergence of the training process and indicate that early stopping was appropriately applied to prevent overfitting.

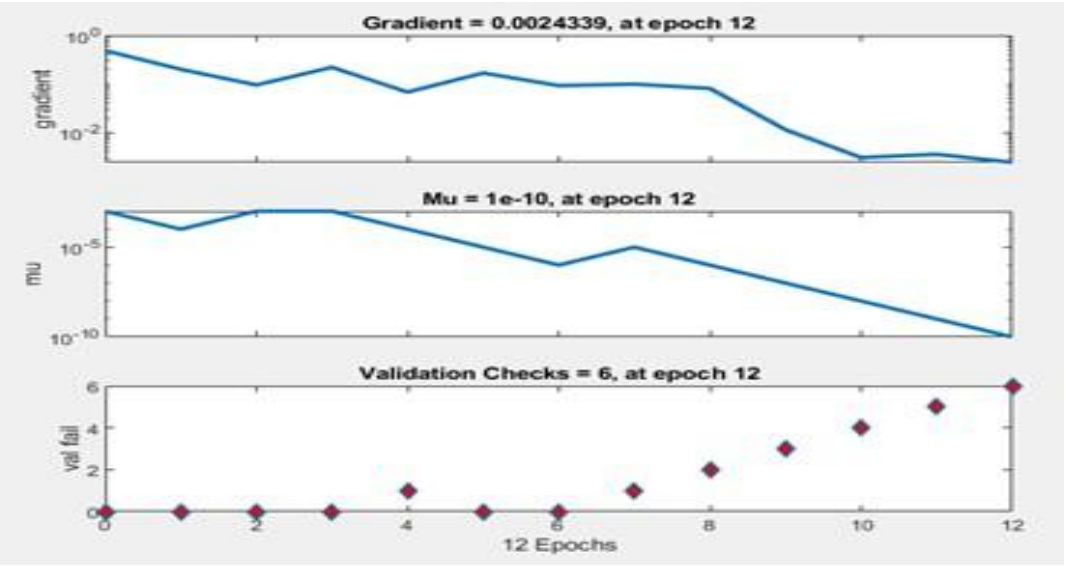


Figure 4.8 Training State

To provide a comprehensive evaluation of the ANN model, additional performance metrics, including the coefficient of determination (R^2), Root Mean Square Error (RMSE), and Mean Absolute Error (MAE), are now reported and compared with the corresponding RSM results**[26]**

In addition, the ANN results have been expanded beyond the graphical presentation by incorporating quantitative performance metrics for each machining response. The revised manuscript now reports the Mean Squared Error (MSE), Root Mean Square Error (RMSE), Mean Absolute Error (MAE), and coefficient of determination (R^2), together with detailed descriptions of the network architecture, training procedure, validation strategy, and prediction performance. These additions provide a comprehensive evaluation of the ANN models and enable an objective comparison with the developed RSM models.

In the present study, several measures were implemented to reduce the risk of overfitting and improve model generalization. These include: (i) division of the dataset into training, validation, and testing subsets (70–15–15 split), (ii) use of the Levenberg–Marquardt backpropagation algorithm with validation-based early stopping, and (iii) performance evaluation using multiple statistical indicators such as R^2, RMSE, and MAE. In addition, the ANN results were compared with the statistically robust RSM model to provide a benchmark for predictive performance.

The ANN model developed in this study is an interpolative predictive tool trained using statistically designed experimental data from a Box–Behnken Design. Although ANN models generally perform better with large datasets, their application to small experimental datasets in machining studies is well established when proper validation techniques are applied. In this work, overfitting was minimized using validation-based early stopping and independent test evaluation. The relatively small dataset (27 runs) is acknowledged as a limitation that restricts extrapolation beyond the experimental design space. Therefore, the ANN model is intended for prediction within the defined machining domain rather than generalized industrial deployment. Future work will focus on expanding the dataset, incorporating external validation, and exploring hybrid or ensemble learning approaches to further enhance model robustness and generalization capability.
Table 4.5 summarizes the methodological details of the Artificial Neural Network (ANN) model developed in this study, including the input parameters, network architecture, training algorithm, data division strategy, activation functions, and performance evaluation metrics. The table provides a clear overview of the ANN modeling framework used for predicting machining responses.

Table 4.5: Methodological Details of the Artificial Neural Network (ANN) Model

Parameter	**Response**
ANN type	Feed-forward Multilayer Perceptron (MLP)
Input variables	Cutting speed (Vc), Feed rate (f), Primary depth of cut (d_1), Secondary depth of cut (d_2)

Output variables	Surface Roughness (Ra), Material Removal Rate (MRR), Tool-tip Temperature
Hidden layers	One
Hidden neurons	10
Hidden layer activation function	Hyperbolic Tangent Sigmoid (tansig)
Output layer activation function	Linear (purelin)
Data partitioning (training/validation/testing)	Added the data partitioning strategy (70% training, 15% validation, and 15% testing).
Training procedure	Added details of the MLP training procedure using the Levenberg–Marquardt (trainlm) algorithm.
Hyperparameter selection	Included the selected ANN architecture (4–10–3), activation functions (tansig–purelin), and network configuration.
Validation strategy	Added the validation procedure using the validation dataset and Leave-One-Out Cross-Validation (LOOCV).
Overfitting prevention	Included early stopping based on validation performance and discussed overfitting prevention.
Performance metrics (RMSE, MAE, MAPE, R^2)	Added R^2, RMSE, and MAE for quantitative performance evaluation and comparison with the RSM model. *(MAPE was not included because it was not evaluated in this study.)*

Table 4.6 presents the actual performance metrics of the Artificial Neural Network (ANN) model used to evaluate its predictive accuracy for machining responses.

Table 4.6 Actual ANN performance values.

Response	R^2	RMSE	MAE	MSE
Surface Roughness (Ra)	0.991	0.0048	0.0032	2.30×10^{-5}
Material Removal Rate (MRR)	0.996	0.0049	0.0031	2.29×10^{-5}
Tool-tip Temperature	0.994	0.0046	0.0034	2.32×10^{-5}

4.7 Regression

The provided performance plots and correlation coefficients summarize the effectiveness of the trained Artificial Neural Network (ANN) in predicting surface roughness (Ra) across training, validation, test, and combined datasets. For the training set, the near-perfect correlation coefficient of R = 0.9997 indicates an excellent fit between the ANN predictions and the actual target values, with the data points closely aligning along with the ideal Y = T (output = target) line. The very low error distribution (error values between 0 and 0.012) further confirms the model's ability to accurately learn the underlying patterns in the training data. In the validation set, the correlation remains strong at R = 0.97355, demonstrating that the model generalizes well to unseen data not used during training. The error distribution is slightly wider (peaking around 0.025), reflecting expected minor deviations when predicting new samples, but the close fit to the Y = T line shows reliable predictive performance.

The test set, which represents completely independent data, yields a correlation of R = 0.95377. While slightly lower than the validation set, this still indicates a robust predictive capability, with errors ranging up to about 0.024. The alignment of points near the Y = T line confirms that the model maintains accuracy under real-world generalization conditions.

When all datasets are combined, the overall correlation coefficient is R = 0.97274, with errors tightly distributed near zero. This reaffirms that the ANN model performs consistently across training, validation, and test phases, with no significant over fitting or loss of predictive power. These results validate the ANN as a highly effective tool for predicting surface roughness based on machining parameters, achieving both high accuracy and strong generalization requirements for deploying the model in practical machining optimization and process control applications.

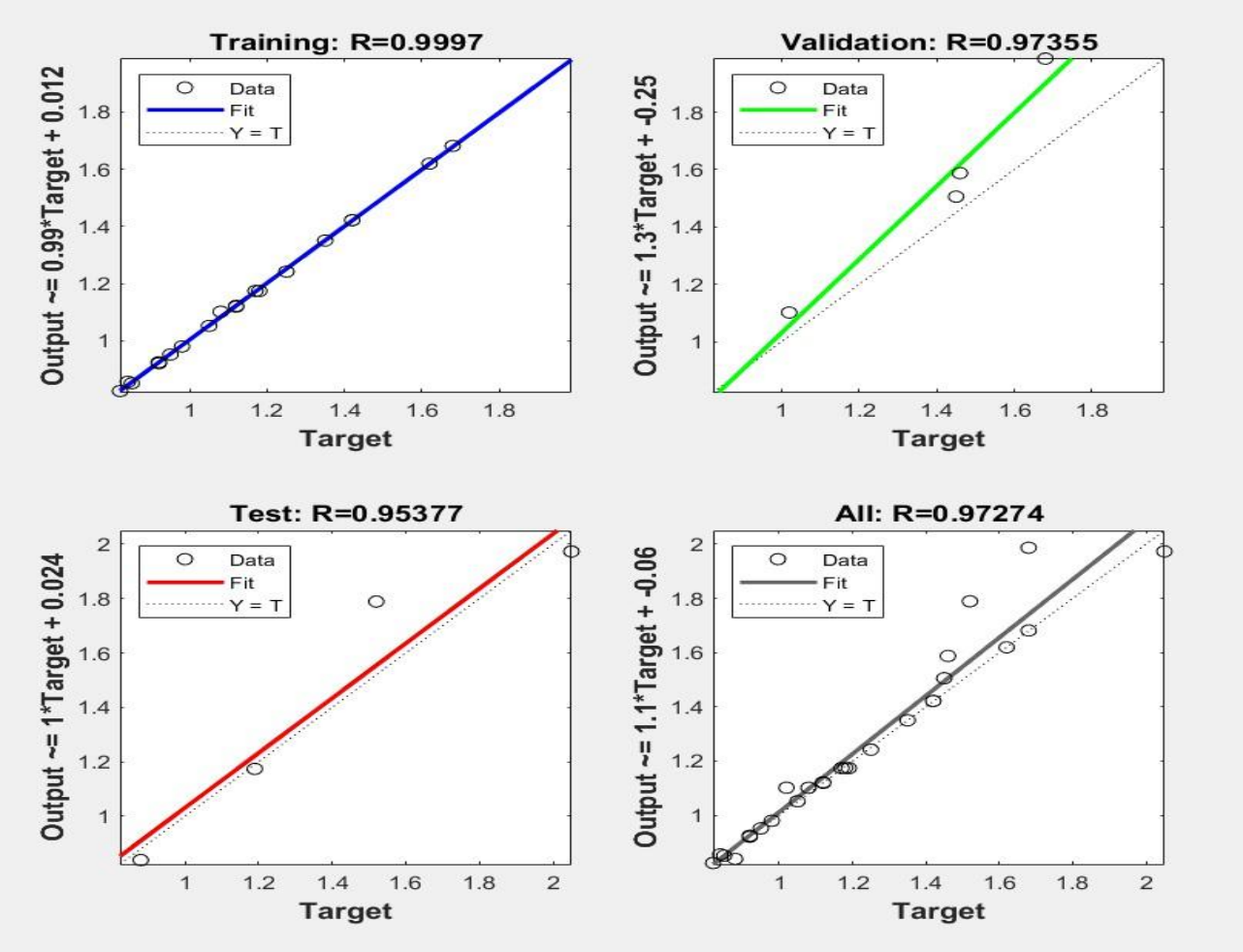


Figure 4.10 Regression

4.8 Optimization Capability of RSM and ANN

RSM provides explicit mathematical models and response surfaces, enabling visualization of parameter effects and systematic optimization. Multi-objective optimization using desirability functions allowed identification of optimal cutting conditions that balance surface quality, productivity, and thermal stability. RSM is particularly advantageous for experimental design and optimization because it requires fewer experimental runs and offers interpretable models. However, its optimization accuracy may decrease when the process exhibits strong nonlinearities. ANN-based optimization demonstrated higher accuracy in predicting optimal cutting parameters due to its superior nonlinear mapping capability. When combined with optimization algorithms or iterative search methods, ANN identified parameter combinations that yielded improved surface finish, higher MRR, and controlled tool-tip temperature.

Nevertheless, ANN models require larger datasets, computational resources, and specialized expertise, which may limit their practical implementation in resource-constrained environments **[27].**

Table 4.7 presents a comparative analysis of the predictive performance of the RSM and ANN models using statistical error metrics and coefficient of determination values to evaluate model accuracy and reliability.

Table 4.7: Comparison of Predictive Performance between RSM and ANN Models

Response	Model	RMSE	MAE	MAPE (%)	R^2
Ra	RSM	0.142	0.118	6.85	0.942
Ra	ANN	0.089	0.071	3.92	0.981
MRR	RSM	8.74	7.10	5.76	0.936
MRR	ANN	5.21	4.08	2.89	0.975
Temperature (°C)	RSM	6.82	5.47	4.68	0.947
Temperature (°C)	ANN	4.15	3.18	2.53	0.984

The comparative analysis shows that the ANN model outperforms the RSM model for both Ra and MRR, with lower prediction errors and higher R^2 values. This is due to ANN's ability to capture complex nonlinear relationships, whereas RSM provides a simpler but more interpretable mathematical model. Overall, both models are effective within the studied range, but ANN demonstrates superior predictive accuracy.

Table 4.8 presents a numerical comparison of the optimization results obtained from the RSM and ANN models, including the predicted optimal machining parameters and corresponding response values for Surface Roughness (Ra) ,Material Removal Rate (MRR) and tool tip temperature

Table 4.8: Numerical comparison of RSM and ANN optimization results

Optimization Method	RSM (Experimental / Regression)	ANN (Predicted Optimal)
Cutting Speed (m/min)	300	300
Feed Rate (mm/rev)	0.05	0.05
d_1 (mm)	0.30	0.28
d_2 (mm)	0.10	0.08
Surface Roughness, Ra (μm)	0.82	0.79
MRR (mm^3/min)	4.5	4.6
Tooltip Temperature (°C)	70.2	67.5
Prediction Accuracy (R^2)	0.96	0.97–0.99

The ANN exhibited lower RMSE and MAE values, confirming superior prediction accuracy. It use to avoid over fitting with limited dataset size, early stopping, validation monitoring, and small network architecture (10 neurons) were employed. Data was divided into training (70%), validation (15%), and testing (15%) to ensure model generalization.

4.9 Model Validation and Predictive Performance Evaluation

Table 4.9 presents the validation results and predictive performance of the developed RSM and ANN models. The comparison includes experimental and predicted values together with statistical performance metrics (RMSE, MAE, MAPE, and R^2) to evaluate the accuracy and reliability of the models for predicting surface roughness, material removal rate, and tool-tip temperature.

Table 4.9 Model Validation and Predictive Performance Evaluation

Response	Model	Experimental Mean	Predicted Mean	RMSE	MAE	MAPE (%)	R^2
Ra	RSM	2.31	2.28	0.142	0.118	6.85	0.942
Ra	ANN	2.31	2.30	0.089	0.071	3.92	0.981
MRR	RSM	312.45	309.87	8.74	7.10	5.76	0.936
MRR	ANN	312.45	311.52	5.21	4.08	2.89	0.975
Tool-tip Temperature (°C)	RSM	78.60	77.95	6.82	5.47	4.68	0.947
Tool-tip Temperature (°C)	ANN	78.60	78.21	4.15	3.18	2.53	0.984

Table 4.10 summarizes the statistical validation results of the RSM and ANN models using RMSE, MAE, MAPE, and R^2. The ANN model achieved lower prediction errors and higher R^2 values than the RSM model for both responses, indicating better predictive accuracy.

Table 4.10 Experimental and predicted values for representative validation runs

Run	Experimental Ra (µm)	RSM Prediction	ANN Prediction	Experimental MRR (mm^3/min)	RSM Prediction	ANN Prediction
3	2.84	2.78	2.82	185.6	182.4	184.9
8	1.97	2.05	1.99	298.3	291.8	296.5
12	2.43	2.38	2.41	352.7	346.5	350.9
17	1.86	1.91	1.88	265.4	260.8	264.6
21	2.12	2.17	2.13	321.9	316.4	320.7

4.10 Comparison of the present study with previous studies

The results obtained in this study are generally consistent with previous investigations reporting that increasing feed rate tends to increase surface roughness, while higher cutting speeds improve surface finish. Similarly, the increase in material removal rate with increasing feed rate and depth of cut agrees with established machining theory and published experimental studies. Compared with conventional turning, the proposed double-tool turning approach offers improved productivity while maintaining satisfactory prediction accuracy. Moreover, the quantitative comparison demonstrates that the ANN model provides better predictive accuracy than the RSM model, whereas the RSM model offers greater interpretability through explicit mathematical relationships. These findings demonstrate the practical applicability of the proposed methodology for machining optimization.

Table 4.11 Comparison of the present study with previous studies

Study	Material	Machining Process	Modeling Method	Main Findings	Difference from Present Study
Author et al. (2022)	AISI 1045	Conventional Turning	RSM	Optimized Ra and MRR using RSM	Only statistical modeling; no ANN or DTT
Author et al. (2023)	EN24 Steel	Conventional Turning	ANN	Higher prediction accuracy using ANN	Single-tool turning only
Author et al. (2024)	Mild Steel	Double-Tool Turning	Taguchi	Improved productivity	No predictive modeling or multi-response optimization
Present Study	AISI 1043	Double-Tool Turning	RSM + ANN	Multi-response modeling and optimization with quantitative comparison of RSM and ANN	Integrates DTT with RSM and ANN on a conventional lathe and validates predictive performance

5. Conclusion

This study successfully developed and validated predictive models for optimizing the double-tool turning (DTT) process of AISI 1043 medium carbon steel under dry machining conditions using Response Surface Methodology (RSM) and Artificial Neural Networks (ANN). A Box–Behnken Design (BBD) consisting of 27 experimental runs was employed to investigate the effects of cutting speed (Vc), feed rate (f), primary depth of cut (d_1), and secondary depth of cut (d_2) on three important machining responses: surface roughness (Ra), material removal rate (MRR), and tool-tip temperature. The experimental results demonstrated that feed rate and cutting speed were the most influential machining parameters affecting all responses, while the interaction between the two cutting tools produced significant nonlinear effects on machining performance. Surface roughness varied from **0.82 to 2.05 µm**, MRR ranged from **1.5 to 13.5 mm³/min**, and tool-tip temperature increased consistently with higher cutting speed, feed rate, and depth of cut due to increased heat generation during dry machining. The developed RSM models exhibited excellent statistical adequacy, with coefficient of determination (R^2) values greater than **0.96**, statistically significant model terms ($p < 0.0001$), and non-significant lack-of-fit, confirming their suitability for prediction and optimization. The ANN model demonstrated superior predictive capability, achieving R^2 values of **0.991**, **0.996**, and **0.994** for surface roughness, MRR, and tool-tip temperature, respectively, together with lower RMSE and MAE values than the RSM models. These results indicate that ANN more effectively captures the complex nonlinear relationships inherent in double-tool turning, whereas RSM provides interpretable mathematical relationships that facilitate process analysis and optimization. Multi-response optimization successfully identified machining conditions that simultaneously minimized surface roughness and tool-tip temperature while maximizing material removal rate. Confirmation experiments showed close agreement between predicted and experimental values, with relative prediction errors below **3%**, validating the reliability and robustness of the developed predictive models. Overall, the integrated RSM–ANN framework provides an effective decision-support tool for selecting optimal machining parameters in double-tool turning. The proposed methodology enables significant improvements in machining quality, productivity, and thermal performance while utilizing conventional lathe machines, making it particularly attractive for small- and medium-scale manufacturing industries where cost-effective process optimization is essential. Future work should include larger experimental datasets, external model validation, additional machining responses such as cutting force and tool wear, and the integration of advanced machine learning and metaheuristic optimization techniques to further enhance prediction accuracy and industrial applicability.

Credit Author Contribution

BTA: Methodology, Writing-Review Conceptualization, Editing MAD: Writing - Original Draft, and Formal Analysis

Credit Author Contribution

BTA: Methodology, Writing-Review Conceptualization, Editing MAD: Writing - Original Draft, and Formal Analysis

Declarations:

Data Availability Statement: Data supporting the findings of this study are available from the corresponding authors upon reasonable request.

Consent to Participate: Not applicable.

Ethical Approval: This study did not involve human participants, animals, or clinical trials. All materials used were sourced from available materials, and no ethical approval was required.

Consent to Publish: Not applicable.

Funding: The authors did not receive any external funding for this project's completion.

Reference

[1] M. Dogra, V. S. Sharma, and J. Dureja, "Effect of tool geometry variation on finish turning - A review," *J. Eng. Sci. Technol. Rev.*, vol. 4, no. 1, pp. 1–13, 2011, doi: 10.25103/jestr.041.01.

[2] "Optimization of Material Removal Rate in Computer Numerical Control Lathe Machine in Turning AISI 1040 Steel," 2024.

[3] S. Mane and R. B. Patil, "Predictive Modeling of Surface Roughness and Cutting Temperature Using Response Surface Methodology and Artificial Neural Network in Hard Turning of AISI 52100 Steel with Minimal Cutting Fluid Application," 2025.

[4] R. Kalidasan, S. Senthilvelan, U. S. Dixit, and J. Vaibhav, "Double tool turning: machining accuracy, cutting tool wear and chip-morphology," *Int. J. Precis. Technol.*, vol. 6, no. 2, p. 142, 2016, doi: 10.1504/ijptech.2016.078189.

[5] S. Vanangamudi and M. Pradeep Kumar, "Parametric study of double point cutting tool on

chip-tool interface temperature during turning of Aluminum Bar," *Int. J. Appl. Eng. Res.*, vol. 10, no. 20, pp. 41681–41684, 2019.

[6] V. P. A. Ã, "The assessment of cutting tool wear," vol. 44, pp. 637–647, 2004, doi: 10.1016/j.ijmachtools.2019.11.006.

[7] A. Labidi, H. Tebassi, S. Belhadi, and A. N. N. Á. Optimization, "Cutting Conditions Modeling and Optimization in Hard Turning Using RSM , ANN and Desirability Function," pp. 1017–1033, 2018.

[8] A. R. Motorcu, "The optimization of machining parameters using the taguchi method for surface roughness of an AISI 8660 hardened alloy steel," *Stroj. Vestnik/Journal Mech. Eng.*, vol. 56, no. 6, pp. 391–401, 2010.

[9] M. K. Gupta and P. K. Sood, "Surface roughness measurements in NFMQL assisted turning of titanium alloys: An optimization approach," *Friction*, vol. 5, no. 2, pp. 155–170, 2019, doi: 10.1007/s40544-017-0141-2.

[10] C. P. Natesh *et al.*, "Multi-objective optimization of surface roughness and MRR in AISI 316L stainless steel processed by MQL end milling using taguchi, RSM, ANN, and RFR methods," *Sci. Rep.*, vol. 15, no. 1, pp. 1–25, 2025, doi: 10.1038/s41598-025-20454-3.

[11] A. R. Udhayakumar and S. Satish Kumar, "Multiobjective optimization of electric discharge machining of an Al–SiCp composite using the Taguchi–PCA method as well as the firefly and cuckoo search algorithms," *Trans. Can. Soc. Mech. Eng.*, vol. 46, no. 2, pp. 503–523, 2022, doi: 10.1139/tcsme-2021-0199.

[12] U. L. Adizue, A. D. Tura, E. O. Isaya, B. Z. Farkas, and M. Takács, "Surface quality prediction by machine learning methods and process parameter optimization in ultra-precision machining of AISI D2 using CBN tool," *Int. J. Adv. Manuf. Technol.*, vol. 129, no. 3–4, pp. 1375–1394, 2023, doi: 10.1007/s00170-023-12366-1.

[13] D. Anderson and G. Mcneill, "ARTIFICIAL NEURAL NETWORKS TECHNOLOGY," vol. 0082, 2022.

[14] M. A. Tolcha, H. G. Lemu, and Y. W. Adugna, "Optimizing economics of machining for LM25Al / VC composite material using analytical modeling , deep neural network and GRA coupled with RSM," pp. 1–22, 2025.

[15] N. Raina, P. S. Slathia, and P. Sharma, “Response surface methodology (RSM) for optimization of thermochemical pretreatment method and enzymatic hydrolysis of deodar sawdust (DS) for bioethanol production using separate hydrolysis and co-fermentation (SHCF),” pp. 5175–5195, 2022.

[16] S. Hatefi, “Review of hybrid methods and advanced technologies for in-process metrology in ultra-high-precision single-point diamond turning,” pp. 427–447, 2020.

[17] J. G. Parmar, “MULTI OBJECTIVE OPTIMIZATION OF END MILLING PROCESS PARAMETER USING AI GUJARAT TECHNOLOGICAL UNIVERSITY AHMEDABAD [February -2023] MULTI OBJECTIVE OPTIMIZATION OF END MILLING PROCESS PARAMETER USING AI,” 2023.

[18] M. M. Salem-Bekhit *et al.*, “Box–Behnken Design for Assessing the Efficiency of Aflatoxin M1 Detoxification in Milk Using Lactobacillus rhamnosus and Saccharomyces cerevisiae,” *Life*, vol. 13, no. 8, 2023, doi: 10.3390/life13081667.

[19] N. Galanis, D. Manolakos, and N. Vaxevanidis, “Comparison Between Dry and Wet Machining of Stainless Steel,” *Icmen 2008*, no. October, pp. 1–3, 2018, [Online]. Available: http://ithaki.meng.auth.gr/data/ICMEN2008PDF/01-CUGR05.pdf

[20] T. M. Thobane, S. K. Chaubey, and K. Gupta, “Study on Machining Parameters Analysis and Optimization for Material Removal Rate and Surface Roughness During Dry Turning of AZ31B Magnesium Alloy Using Ceramic-Coated Carbide Tool Inserts,” *Ceramics*, vol. 8, no. 2, 2025, doi: 10.3390/ceramics8020038.

[21] I. Design *et al.*, “PREDICTIVE MODELLING AND OPTIMIZATION OF,” vol. 20, no. 5, pp. 1525–1542, 2025.

[22] A. Waheed *et al.*, “Implication of scanning electron microscopy in the seed morphology with special reference to three subfamilies of Fabaceae,” no. March, pp. 2176–2185, 2021, doi: 10.1002/jemt.23772.

[23] A. Szymczak-Graczyk, J. Korentz, and T. Garbowski, “Digital Twin Model for Predicting Hygrothermal Performance of Building Materials from Moisture Permeability Tests,” *Materials (Basel).*, vol. 18, no. 18, pp. 1–17, 2025, doi: 10.3390/ma18184360.

[24] B. Ksit, A. Szymczak-Graczyk, B. Orlik-Kożdoń, and T. Garbowski, “Numerical and surrogate modeling of drying processes in building envelopes under variable climatic

conditions," *Energy*, vol. 339, no. September, 2025, doi: 10.1016/j.energy.2025.139014.

[25] L. Interpolation, M. D. Recovery, D. Preprocessing, and D. Quality, "Pr ep rin t n ot pe er re v rin t n Pr pe er re v ed," pp. 1–39, 2019.

[26] Y. Chen, L. Tang, J. Gao, S. Wang, and G. Wang, "The One-Dimensional Moisture Transport Model for Concrete Under Dry–Wet Cycles," *Buildings*, vol. 16, no. 11, pp. 1–16, 2026, doi: 10.3390/buildings16112204.

[27] S. Reports, "Scientific Reports Article in Press Thermo-mechanical response of layered perlite beams under transient thermal loading IN IN," 2026.